Thermal and plastic behavior of nanoglasses

Oliver Franke[a)]
Department of Aerospace and Mechanical Engineering and The Mork Family Department for Chemical Engineering and Materials Science, University of Southern California, Los Angeles, California 90089

Daniel Leisen
Institute for Applied Materials, Karlsruhe Institute of Technology (KIT), 76344 Eggenstein-Leopoldshafen, Germany

Herbert Gleiter
Herbert Gleiter Institute of Nanoscience of the Nanjing University of Science and Technology, Nanjing, China; and Institute for Nanotechnology, Karlsruhe Institute of Technology (KIT), 76344 Eggenstein-Leopoldshafen, Germany

Horst Hahn
Institute for Nanotechnology, Karlsruhe Institute of Technology (KIT), Eggenstein-Leopoldshafen, Germany; and KIT-TUD Joint Research Laboratory Nanomaterials, Institute of Materials Science, Technische Universitaet Darmstadt (TUD), 64287 Darmstadt, Germany

(Received 1 October 2013; accepted 29 April 2014)

The mechanical and thermal behavior of nanoglasses (NGs) were studied with a focus on the effect of the microstructure. The thermal expansion was measured to track changes in excess free volume during heating. It was found that the excess free volume, which is initially more dominant in the interphase region between the denser amorphous particles, is partially lost as well as redistributed during annealing. This relaxation during heating causes the nanoglass to behave like a melt-spun ribbon after heating while remaining amorphous. Nanomechanical tests were used to probe the local incipient plasticity and the influence of the interphase region. This interphase appears to affect the mechanical response of the NGs by inhibiting the propagation of shear bands and thus offers a novel approach for the introduction of plasticity in bulk metallic glasses. The results suggest that the NGs consist of two distinct amorphous phases with different glass transition temperatures.

I. INTRODUCTION

Nanoglasses (NGs) constitute a new subcategory of amorphous materials with a wide range of interesting properties including changes in their magnetic and mechanical behavior.[1] While regular metallic glasses are obtained by freezing the liquid state in a quenching or rapid cooling process. NGs are created by inert gas condensation leading to small amorphous particulates that can be compressed and "sintered" into a bulk material.[1–4] NGs can also be generated by severe plastic deformation of bulk metallic glasses (BMGs)[5] and recently by magnetron sputtering using powder targets.[6] It was found experimentally that NGs exhibit a higher intermediate range order than BMGs.[3] Molecular dynamics (MD) simulations and experimental results for NG structures revealed that the interphase region between the particles contains a significantly larger fraction of excess free volume than the particles,[2,7,8] which is considered to be the main reason for the changed response of the material.

Typical BMGs usually fail catastrophically by shear banding once a critical stress is surpassed.[9–11] Once the so-called shear transition zones are activated, their avalanche-like propagation creates the shear bands.[12] This rapid shear banding destroys the short-range order (SRO) of the BMGs during its progress.[12] The absence of a mechanism to inhibit or slow the shear bands leads to lack of damage tolerance and limited plasticity,[11,13–15] thus severely limiting their applicability. In contrast, NGs were found to have a lower yield strength than typical BMGs, but exhibited plastic deformation while having a comparable fracture strength.[2] This unusual behavior was attributed to the intersection of multiple shear bands at the interface.[2]

Although several approaches have been taken to enhance the plasticity in BMGs,[14–16] the underlying understanding of how to stop the propagation of shear bands is still needed. However, due to the premature failure of BMGs (as opposed to NGs), the first shear band or set of parallel shear bands in an unconfined volume usually leads to catastrophic failure at room temperature thus limiting further studies of shear band interaction.

Shear bands can be considered to be either a sequence of shear transformation zones (STZ) being activated[12] or a discrete burst after intense strains have been accumulated

[a)]Address all correspondence to this author.
e-mail: ofranke@usc.edu
DOI: 10.1557/jmr.2014.101

 © Materials Research Society 2014

https://doi.org/10.1557/jmr.2014.101 Published online by Cambridge University Press

in a confined volume.[11] While the true mechanism is likely to be in between those two extremes,[11] both mechanism will lead to the creation of extra free volume and destruction of SRO.[11,12,17,18] Ritter et al. showed that the interphase region in the NGs exhibits the properties of a shear band[7] and thus has a destroyed SRO.[18–20] It was also found that annealing/relaxation of BMGs can recreate the SRO to some extent.[19,21,22] For example, it was reported that in a Cu–Zr-system, a disturbed SRO can decrease the modulus of metallic glasses.[23] Koebrugge et al. found that SRO increases the modulus and discovered that relaxed glasses will have higher moduli.[22] Chen et al. measured an increase in the modulus for sputtered Au-NG.[24]

These results are important as the work presented in this paper basically encounters both phenomena, a constant and an increased modulus. It will be shown that signs of two distinct regions are in fact present in NGs and are contributing to the mechanical response. Since NGs contain large volume fractions of both the amorphous shearband-like interphase region and the amorphous particulates,[1,8,25] this leads to a two-phased material with two distinct glass transition temperatures. This two-phased microstructure could be used to introduce plasticity in amorphous materials.

II. EXPERIMENTAL DETAILS

Two nanoglass pellets of the nominal composition $Fe_{28}Sc_{72}$ and $Fe_{90}Sc_{10}$, respectively, as well as two melt-spun ribbon samples of $Fe_{24}Sc_{76}$ and $Fe_{90}Sc_{10}$, were investigated. The procedure for the sample preparation via inert gas condensation can be found elsewhere.[1,3,4,25] To obtain compact samples for mechanical testing, all pellets were compressed at 5 GPa. Each pellet was used to obtain multiple samples for both indentation and thermal expansion coefficient measurements. The samples used for the nanoindentation experiments were polished to a mirror finish while the samples used for the thermal expansion measurements underwent both indentation and thermal expansion analysis.

Nanoindentation tests were performed using both a MTS XP Nanoindenter (Agilant, Phoenix, AZ) and Hysitron Triboindenter (Hysitron, Eden-Prairie, MN). Experiments in the MTS Indenter were performed using a depth-limited thin film method with continuous stiffness measurement (CSM) and a maximum displacement of 200 nm at a strain rate of 0.05 s^{-1}. The experiments in the Triboindenter were performed under load control with a maximum load of 5000 N to achieve the same maximum displacement. Arrays of 25–49 indents were performed for each condition and sample with a minimum spacing of 4 μm between indents to avoid interference by previous indents.

Thermal expansion was measured for the Fe-rich samples only using a custom apparatus using a modified digital image correlation (DIC) code originally developed by Eberl et al.[26] The application of DIC allows for the strain to be measured in x and y. A total of 30 images were taken at temperature intervals of 20 °C. For each set of 10 images, an average strain value was determined resulting in three independent strain values for each temperature. Calibration of the set-up was performed by using an aluminum foil of technical purity. The thermal expansion measurements were found to be a good match of literature values. To minimize oxidation all experiments were performed in an inert gas environment.

The temperature profile used for the NGs differs from the simple heating–cooling pattern used for Al and is shown in Fig. 1. It was comprised of two heating segments with an intermittent cooling segment. This was done to verify the reversibility of the thermal expansion and to study the thermal stability of the NGs. The sample was slowly heated to each target temperature, making sure that it did not surpass the target temperature at any time and was equilibrated for several minutes before the images to determine the strain were taken. The reference sample was subjected to the same heat treatment. The nanoglass samples were retested after undergoing one full cycle of thermal expansion measurements.

The chemical composition of both the source material and the final sample was measured using energy dispersive x-ray spectroscopy (EDX) in a JEOL JSM-7001 FE SEM (Jeol Ltd., Tokyo, Japan). X-ray diffraction analysis was performed using Rigaku diffractometer (Ultima IV, Rigaku, Japan) before and after the coefficient of thermal expansion (CTE) measurements to verify the amorphous character of the material.

III. RESULTS AND DISCUSSION

A. Thermal behavior

To access and verify that there is a two-phased structure created by the excess free volume in the NGs

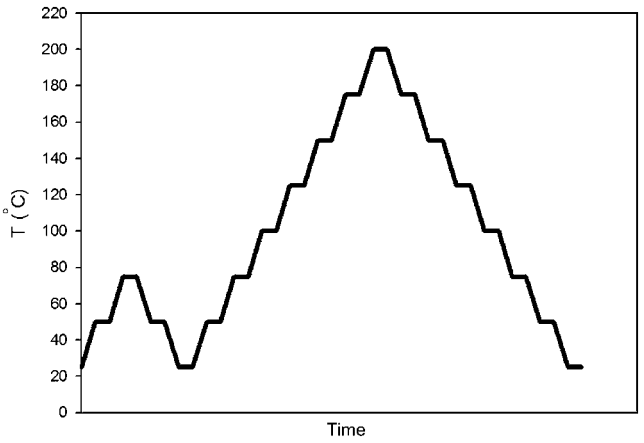


FIG. 1. Temperature–time profile used to measure the thermal expansion behavior of the NG (note that the time increments vary in duration as the prime objective is to avoid exceeding the target temperature).

https://doi.org/10.1557/jmr.2014.101 Published online by Cambridge University Press

and that this second phase has properties similar to a shear band, a series of thermal measurements were conducted using both NGs and standard BMGs ribbons of the same composition. In Fig. 2(a), the strain–temperature diagrams for the NGs show that in the low T-regime ($T < 100$ °C) the material is expanding and the strain is fully recovered upon cooling in both the x- and y-direction. Neither the sample location (center versus edge of the pellet) nor the strain direction showed significant change in the response. Once the material is heated all the way to the maximum temperature of 200 °C, the strain stays constant and becomes negative upon cooling to room temperature (RT). For the ribbons, regular thermal expansion upon heating and contraction upon cooling with a net strain of approximately zero is observed [Fig. 2(b)]. After a second run on the NGs, their behavior was found to be similar to the reference ribbons [Fig. 2(b)]. Figures 3(a) and 3(b) show the total thermal strain (red lines with circles) and the difference between the total strain and the thermal strain originating from expansion. The thermal expansion strain was calculated based on the assumption that pure thermal expansion is fully reversible and that all other contributions to the total strain are caused by structural changes in the material. Following this approach, the thermal contraction data were used to extract the reversible thermal strain to be subtracted from the total strain. The result of this calculation is shown in Figs. 3(a) and 3(b) (blue line with squares). The change in free volume can be calculated assuming an isotropic behavior and taking the average of the x- and y-strain as z-strain, a volume strain V/V_0 of 10^{-8} can be computed for the NG.

Our results from the thermal expansion experiments show that the heat treatment involved does not crystallize the material (verified by XRD; data not shown here). However, there appears to be a significant release and redistribution of the excess free volume, ultimately

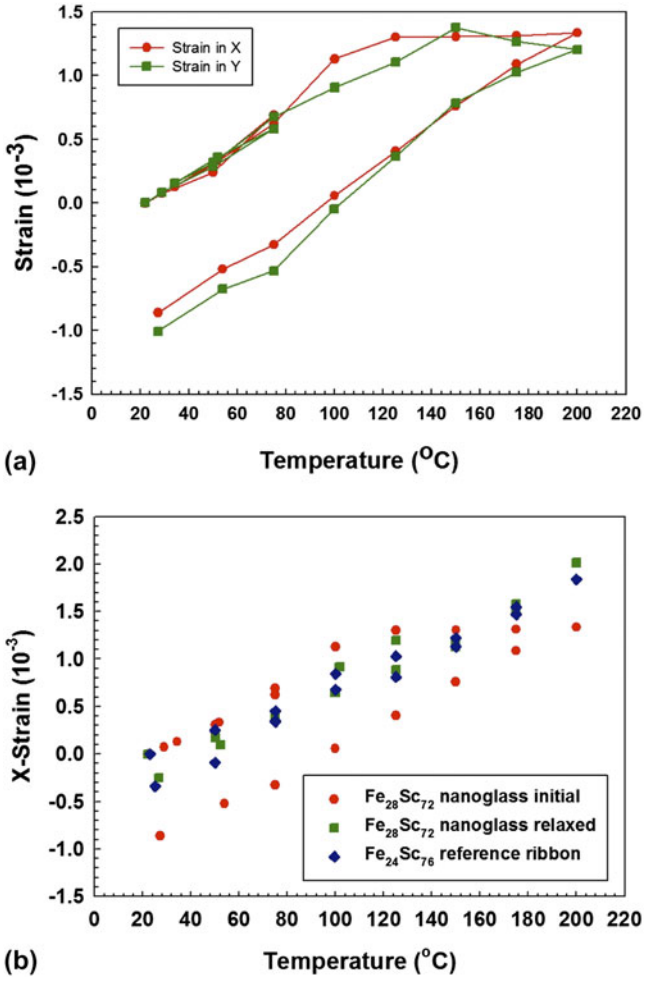


FIG. 2. (a) Strain plot for the NG in x- and y-direction as a function of temperature (b) comparison of strain for the BMG to the NG in its initial state and after one cycle of thermal expansion measurements.

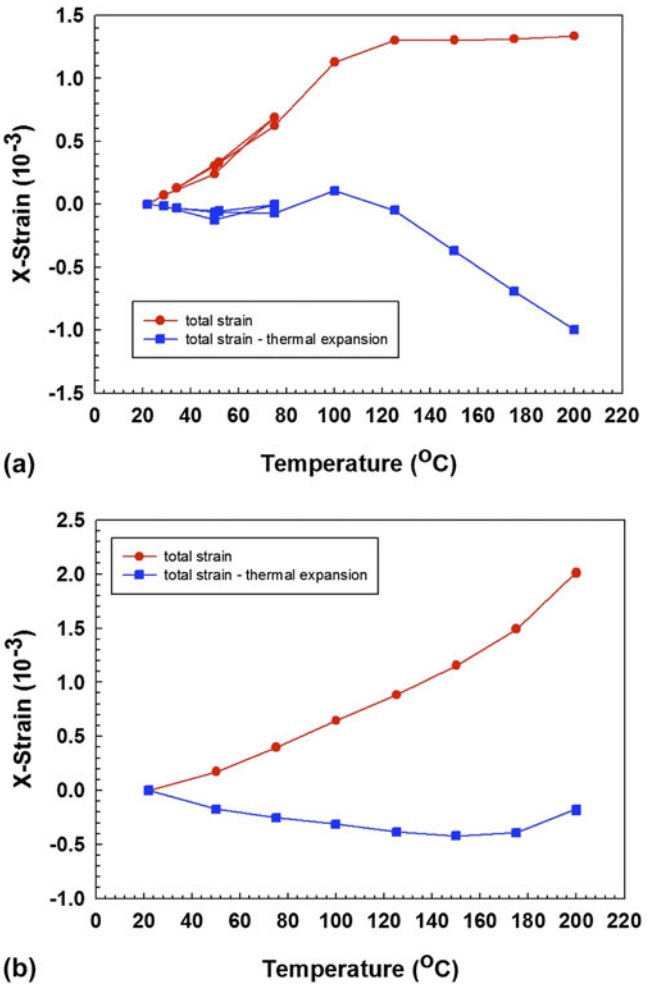


FIG. 3. Thermal strain in the x-direction for the $Fe_{25}Sc_{75}$ NG and the lost volume for the initial run (a) and after one round of thermal expansion measurements (b). The blue line with squares indicates the irreversible thermal strain contribution as obtained from thermal contraction subtracted from the total thermal strain.

https://doi.org/10.1557/jmr.2014.101 Published online by Cambridge University Press

causing the sample to shrink throughout the experiment. This behavior matches the thermal expansion measured in severely deformed BMGs.[27] Given that the excess free volume in the interphase region was found to be in excess of 15%,[24,28] it appears that this relaxation of the material possibly correlates with a redistribution of the excess free volume in the interphase region. The higher than usual excess free volume is formed by an inverse sintering process (where the porosity is absorbed into the material rather than material being diffused to fill the voids like in a regular sintering process encountered in crystalline solids). This mechanism is only available as the material is still in its liquid-like state and can absorb excess free volume at the price of a destroyed SRO in the interphase region. Surprisingly, this microstructure is quite stable and a change in excess free volume cannot be observed at temperatures below 100 °C, when a deviation from the previously observed linearity becomes obvious. Once the material is heated beyond this temperature, a homogenization of this metastable state occurs transforming it into a more stable BMG state. This could also be an indication that metallic glasses can actually exist in more than two states. Each state itself is metastable and has its own glass transition temperature. The results from the second run on the NG clearly show that, while the material is still amorphous, there is a good match in the thermal expansion and mechanical behavior of the former NG and the reference BMG. This would mean that our interphase region, which is structurally similar to a shear band, transforms into its more stable state. A similar observation was made on severely deformed BMGs by Yavari et al., who measured a loss of excess free volume in the deformed BMG sample and obtained the same values as for the initial BMG in a second run,[27] further highlighting that our hypothesis of the interphase region behaving similar to shear bands appears to be valid.

The main difference is that this interphase region, which can also be considered a second glassy phase is formed in the manufacturing process. As a consequence, it can be assumed that there are two ways to generate this second phase: (i) processing as for the NGs and (ii) through mechanical activation during deformation as for the BMGs. In regular BMG, shear bands do not relax without thermal activation and are thus thermodynamically metastable at RT.

As a consequence, a NG can be considered a two-phased amorphous material consisting of two distinct glasses that are structurally different but chemically similar. Classical processing techniques such as rapid quenching suggest that there is only one metastable state for each composition. While our results using low temperature processing techniques indicate that there are at least two phases that are metastable under certain conditions much like a crystalline material with two phases that are different in their crystal structure.

B. Mechanical behavior

To further evaluate the effect of free volume, nanoindentation tests were performed on both NGs and ribbons as shown in Figs. 4–6. Reduced modulus and hardness maps were created for both the NG [Figs. 4(a) and 4(c)] and the BMG [Figs. 4(b)–4(d)]. The maps clearly show the variations of the mechanical properties as a function of location indicating that the microstructure is not less homogeneous in the NGs than in the ribbon. For the Sc-rich ($Fe_{25}Sc_{75}$) samples, an increase in hardness as well as modulus is found for the NGs as compared with the melt-spun ribbon samples [Figs. 4(a)–4(d)], while the Fe-rich NGs ($Fe_{90}Sc_{10}$) do not exhibit this difference ($E_{r,NG} = 130.1 \pm 5.9$ GPa, $H_{NG} = 7.0 \pm 0.5$ GPa, $E_{r,BMG} = 138.7 \pm 6.7$ GPa, and $H_{BMG} = 8.2 \pm 0.7$ GPa). Some of the NGs exhibit a significant increase in the modulus and hardness. There are two possible explanations for this increase. Albe et al. recently studied the deformation of NGs using MD simulations.[7,8] Based on their analysis, the interphase region has a comparable structure to shear bands in regular BMGs.[7,8] Even though the excess free volume determined in the simulation does not match the measured values, the concept of the interphase region being equivalent to a shear band seems plausible.[3,7,8,25] This would also mean that the interface region would not only have more excess free volume than the bulk but also a disturbed SRO, which has been shown to decrease the modulus.[22,23] The second option would be a contamination of the NG samples with oxygen in particular, as Sc has a high affinity for oxygen. Even though a similar increase has been observed in sputtered Au-NG,[24] currently contamination with oxygen appears to be the more likely explanation for the increased RT modulus. A $Fe_{28}Sc_{72}$ NG sample tested in technical purity Ar (99.9%) showed a significant increase in modulus [Figs. 5(a) and 5(b)]. Since the increase is in the order of just 25%, SRO-effects during heating in the thermal expansion measurement as an explanation fall short. In particular, considering that while the oxygen contamination was still too low to be quantified by EDX, oxygen peaks were observed after CTE measurements in technical purity Ar (99.9%).

A more significant finding of the current study is the absence of pop-in events indicating shear localization in macroscopic shear bands. Even though the modulus and hardness data are inconclusive in respect to a clear difference between NGs and BMGs, the load–displacement curves for the reference ribbon and the nanoglass sample of the same composition clearly exhibit a different behavior (Fig. 6). While the melt-spun ribbon shows sharp displacement bursts usually attributed to shear localization and heterogeneous deformation by shear banding, it is evident that those pop-in events are missing or are below the displacement resolution of the NI system (Fig. 6). It appears

https://doi.org/10.1557/jmr.2014.101 Published online by Cambridge University Press

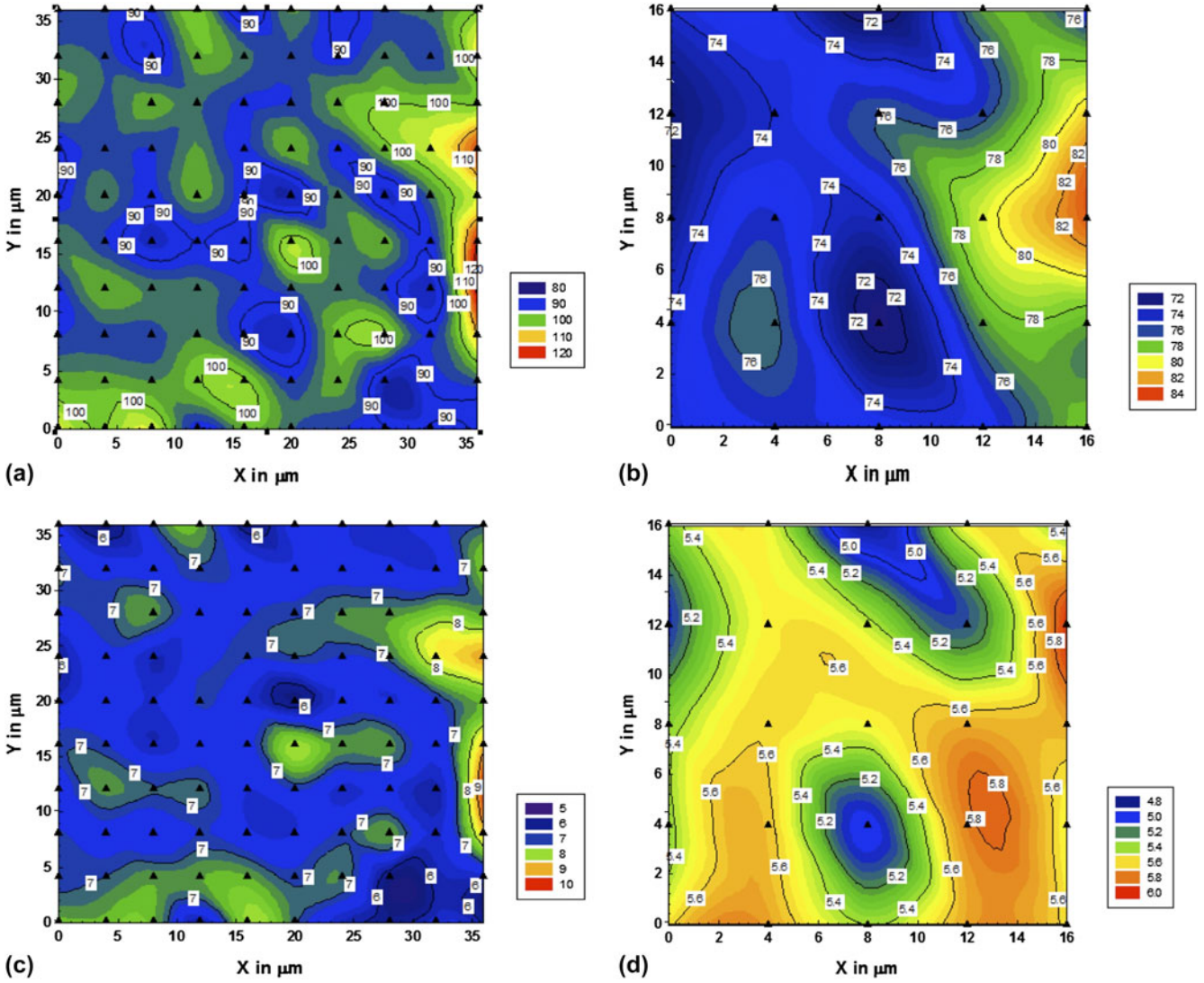


FIG. 4. Modulus E_r and hardness H maps for the $Fe_{25}Sc_{75}$ NG and BMG. Modulus (a) NG, (b) BMG and Hardness, (c) NG, and (d) BMG. Triangles indicate the location of the indents.

that there is yet another change in the incipient plasticity which unlike the ones known so far seems to be not only temperature dependent but also microstructure dependent.

A shear band in a metallic glass is usually formed by the activation of STZ and the development of a coercive avalanche of these STZs until the shear band covers the distance from the surface to the point of the maximum shear stress underneath the indenter.[29,30] The shear bands destroy the SRO in the metallic glasses.[7,18,20,21,31] In the NGs, there are already regions where the SRO is disturbed, namely the interphase region.[7,8]

As discussed in a review by Schuh et al., several studies have investigated primary and secondary shear banding in confined volumes, although these shear bands were either parallel or right on top of each other[11] but did not intersect. It is important to note that in confined loading conditions such as encountered in, for example, nanoindentation or uniaxial compression, multiple shear bands can be initiated in various directions without a complete failure of the sample.[11,13] Nonetheless, they will not intersect during their propagation. A study by Jiang et al. investigated the effect of prestraining BMGs and found an increase in plasticity and strength using indentation[21] due to the intersection of the shear bands.

Consequently, an avalanche of STZs approaching an area of disturbed SRO (interphase/secondary glass phase) will be stopped. There are two analogies that can be used to describe the phenomenon:

(i) The SRO can be considered to be the equivalent of a slip system in a crystal and the interphase region can be treated as a grain boundary (GB). Both the interphase region and the GB are disturbed areas. In conclusion, the motion of the respective carrier of plasticity (the shear

https://doi.org/10.1557/jmr.2014.101 Published online by Cambridge University Press

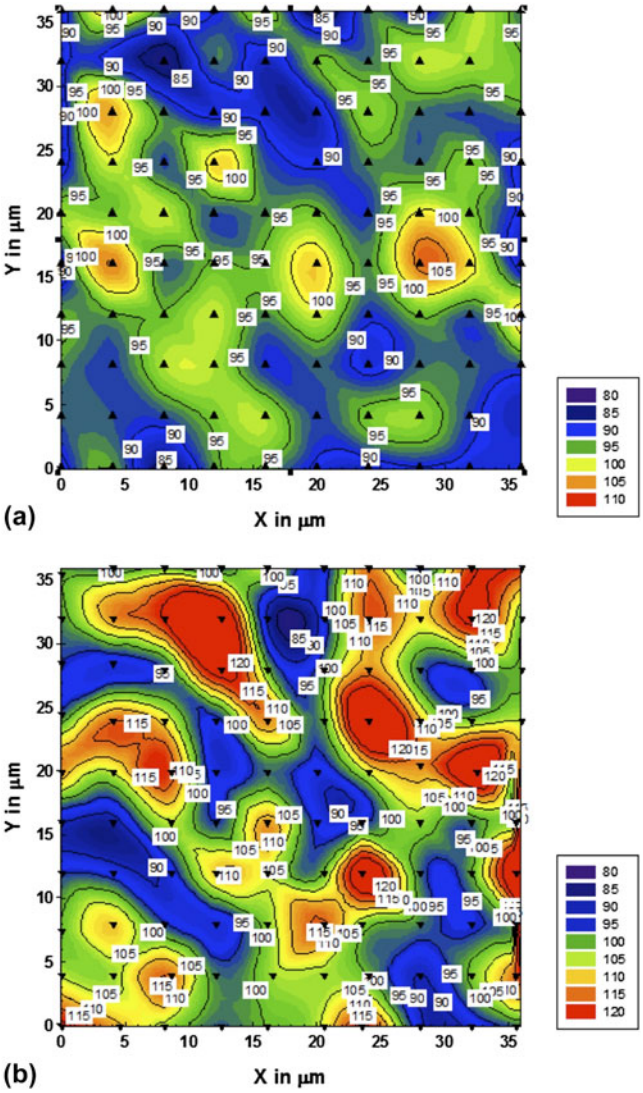


FIG. 5. Modulus map for a $Fe_{28}Sc_{72}$ before (a) and after the thermal expansion measurement (b).

band for the metallic glass and the dislocation for the crystal) will be inhibited.

(ii) Another possible and better analogy is that the shear band feeds of the SRO along the highest stress path destroying it in the process. To stop the propagation of this avalanche, the supply of undestroyed SRO in its path must be eliminated. The interphase potentially provides such an interruption of SRO.

Since the indentation is a mechanically irreversible process, the second analogy (case (ii)) appears to be more suitable. Consequentially, the plastic deformation required to accommodate the indent has to be homogeneously distributed throughout several small amorphous particles. In regular metallic glasses, the transition from highly localized/heterogeneous deformation to a more homogeneous deformation occurs at 0.8 T_g. To our knowledge, this is the first experimental indication that shear bands can be

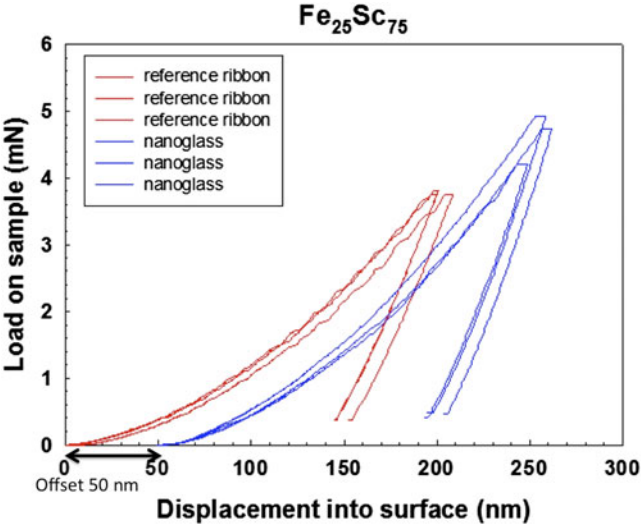


FIG. 6. Representative load–displacement curves for the $Fe_{25}Sc_{75}$ NG and the BMG ribbon.

inhibited by the interphase region in NGs and thus a homogeneous deformation behavior is obtainable in NGs at low temperatures. This opens a new avenue for metallic glasses and also their application in mechanical loading scenarios requiring some plasticity prior to failure.

IV. CONCLUSIONS

In this paper, we were able to show that through microstructural modifications bulk amorphous materials can be tuned to inhibit shear bands. This can mainly be attributed to the presence of a second phase with a disturbed SRO. As the structure is relaxed/heated above the glass transition temperature of the interphase, this interphase region is annihilated by a redistribution of the excess free volume. As a consequence, both the thermal as well as the mechanical behavior exhibit the behavior of a SRO-dominated BMG with regular fluctuations. To understand this transition and the inhibition of the macroscopic shear banding, better parameters such as the particle size, interphase region thickness, and strain rate need to be investigated further.

ACKNOWLEDGMENTS

We would like to thank Dr. Tao Feng (KIT) for preparing the nanoglass samples. The discussions with Dr. Chris Eberl (KIT) on the DIC and Prof. Andrea Hodge (USC) are gratefully acknowledged. We would also like to thank Dr. Ruth Schwaiger (KIT) for providing access to the MTS/Agilent nanoindenter.

REFERENCES

1. M. Ghafari, H. Hahn, H. Gleiter, Y. Sakurai, M. Itou, and S. Kamali: Evidence of itinerant magnetism in a metallic nanoglass. *Appl. Phys. Lett.* **101**(24), 243104 (2012).

https://doi.org/10.1557/jmr.2014.101 Published online by Cambridge University Press

2. J.X. Fang, U. Vainio, W. Puff, R. Wurschum, X.L. Wang, D. Wang, M. Ghafari, F. Jiang, J. Sun, H. Hahn, and H. Gleiter: Atomic structure and structural stability of Sc75Fe25 nanoglasses. *Nano Lett.* **12**(1), 458 (2012).
3. M. Ghafari, S. Kohara, H. Hahn, H. Gleiter, T. Feng, R. Witte, and S. Kamali: Structural investigations of interfaces in Fe90Sc10 nanoglasses using high-energy x-ray diffraction. *Appl. Phys. Lett.* **100**(13), 133111 (2012).
4. H. Gleiter: Nanostructured materials: Basic concepts and microstructure. *Acta Mater.* **48**(1), 1 (2000).
5. X.D. Wang, Q.P. Cao, J.Z. Jiang, H. Franz, J. Schroers, R.Z. Valiev, Y. Ivanisenko, H. Gleiter, and H.J. Fecht: Atomic-level structural modifications induced by severe plastic shear deformation in bulk metallic glasses. *Scr. Mater.* **64**(1), 81 (2011).
6. X.T.S.N. Chen, A. Takeuchi, K.S. Nakayama, H.K. Wu, M. Esashi, A. Inoue, and D.V. Louzguine-Luzgin: A representative of a new class of materials: Nanograined metallic glasses showing unique properties. *AIP Conf. Proc.* **1518**, 682 (2013).
7. Y. Ritter, D. Sopu, H. Gleiter, and K. Albe: Structure, stability and mechanical properties of internal interfaces in Cu64Zr36 nanoglasses studied by MD simulations. *Acta Mater.* **59**(17), 6588 (2011).
8. D. Sopu, K. Albe, Y. Ritter, and H. Gleiter: From nanoglasses to bulk massive glasses. *Appl. Phys. Lett.* **94**(19), 191911 (2009).
9. C.A. Schuh, A.C. Lund, and T.G. Nieh: New regime of homogeneous flow in the deformation map of metallic glasses: elevated temperature nanoindentation experiments and mechanistic modeling. *Acta Mater.* **52**(20), 5879 (2004).
10. C.A. Schuh and T.G. Nieh: A nanoindentation study of serrated flow in bulk metallic glasses. *Acta Mater.* **51**(1), 87 (2003).
11. C.A. Schuh, T.C. Hufnagel, and U. Ramamurty: Mechanical behavior of amorphous alloys. *Acta Mater.* **55**(12), 4067 (2007).
12. A.S. Argon: Plastic-deformation in metallic glasses. *Acta Metall.* **27**(1), 47 (1979).
13. C. Suryanarayana: Mechanical behavior of emerging materials. *Mater. Today* **15**(11), 486 (2012).
14. C.C. Hays, C.P. Kim, and W.L. Johnson: Improved mechanical behavior of bulk metallic glasses containing in situ formed ductile phase dendrite dispersion. *Mater. Sci. Eng., A* **304–306**, 650 (2001).
15. M. Calin, J. Eckert, and L. Schultz: Improved mechanical behavior of Cu–Ti-based bulk metallic glass by in situ formation of nanoscale precipitates. *Scr. Mater.* **48**(6), 653 (2003).
16. J. Eckert, J. Das, S. Pauly, C. Duhamel, K.B. Kim, S. Yi, and W.H. Wang: Impact of microstructural inhomogenities on the ductility of bulk metallic glasses. *Mater. Trans.* **48**(7), 1806 (2007).
17. Y.M. Chen, T. Ohkubo, T. Mukai, and K. Hono: Structure of shear bands in Pd40Ni40P20 bulk metallic glass. *J. Mater. Res.* **24**(1), 1 (2009).
18. Y. Shi and M.L. Falk: Does metallic glass have a backbone? The role of percolating short range order in strength and failure. *Scr. Mater.* **54**(3), 381 (2006).
19. Y. Ritter and K. Albe: Thermal annealing of shear bands in deformed metallic glasses: Recovery mechanisms in Cu64Zr36 studied by molecular dynamics simulations. *Acta Mater.* **59**(18), 7082 (2011).
20. C.A. Pampillo: Localized shear deformation in a glassy metal. *Scr. Metall.* **6**(10), 915 (1972).
21. F.E.P.W.H. Jiang and M. Atzmon: Mechanical behavior of shear bands and the effect of their relaxation in a rolled amorphous Al-based alloy. *Acta Mater.* **53**, 3469 (2005).
22. G.W. Koebrugge, J. Sietsma, and A. van den Beukel: Structural relaxation in amorphous Pd40Ni40P20. *Acta Metall. Mater.* **40**(4), 753 (1992).
23. Y. Shibutani, M. Wakeda, S. Ogata, and J. Park: Computational relationship of deformation behavior and materials strength of amorphous alloys to short-ranged local structures. In *THERMEC 2006, Pts 1-5*, T. Chandra, K. Tsuzaki, M. Militzer, and C. Ravindran eds.; Trans Tech Publications Ltd: Switzerland, 2007, 1911.
24. N. Chen, D.V. Louzguine-Luzgin, G.Q. Xie, P. Sharma, J.H. Perepezko, M. Esashi, A.R. Yavari, and A. Inoue: Structural investigation and mechanical properties of a representative of a new class of materials: nanograined metallic glasses. *Nanotechnology* **24**(4), 045610 (2013).
25. J.X. Fang, U. Vainio, W. Puff, R. Wurschum, X.L. Wang, D. Wang, M. Ghafari, F. Jiang, J. Sun, H. Hahn, and H. Gleiter: Atomic structure and structural stability of Sc75Fe25 nanoglasses. *Nano Lett.* **12**(9), 5058 (2012).
26. C. Eberl, D.S. Gianola, and K.J. Hemker: Mechanical characterization of coatings using microbeam bending and digital image correlation techniques. *Exp. Mech.* **50**(1), 85 (2010).
27. A.R. Yavari, A.L. Moulec, A. Inoue, N. Nishiyama, N. Lupu, E. Matsubara, W.J. Botta, G. Vaughan, M. Di Michiel, and Ö. Kvick: Excess free volume in metallic glasses measured by x-ray diffraction. *Acta Mater.* **53**(6), 1611 (2005).
28. N. Chen, R. Frank, N. Asao, D.V. Louzguine-Luzgin, P. Sharma, J.Q. Wang, G.Q. Xie, Y. Ishikawa, N. Hatakeyama, Y.C. Lin, M. Esashi, Y. Yamamoto, and A. Inoue: Formation and properties of Au-based nanograined metallic glasses. *Acta Mater.* **59**(16), 6433 (2011).
29. C.E. Packard, O. Franke, E.R. Homer, and C.A. Schuh: Nanoscale strength distribution in amorphous versus crystalline metals. *J. Mater. Res.* **25**(12), 2251 (2010).
30. C.E. Packard and C.A. Schuh: Initiation of shear bands near a stress concentration in metallic glass. *Acta Mater.* **55**(16), 5348 (2007).
31. Y.F. Shi and M.L. Falk: Stress-induced structural transformation and shear banding during simulated nanoindentation of a metallic glass. *Acta Mater.* **55**(13), 4317 (2007).

https://doi.org/10.1557/jmr.2014.101 Published online by Cambridge University Press